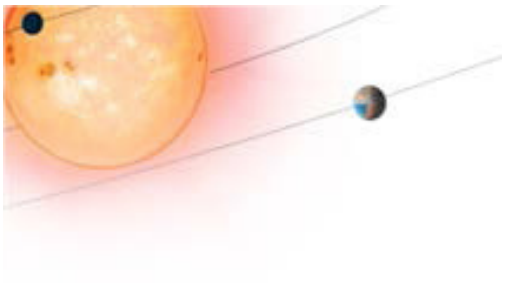

WP 126 100

l'Observatoire de Paris — LESIA

Planetary Transits and Oscillations of Stars PLATO 2.0

PLATO-LESIA-PSPM-TN-014

Issue 1.0 Revision 1.0

The Solar-like Light-curve Simulator (SLS)

Mandatory Cover Page Attributes:

Document Title:	The Solar-like Light-curve Simulator (SLS)
Origin Name:	WP 126 100
WBS code:	N/A
Package code:	N/A

Distribution List

Public	[ ]

Approval Sheet

	Name	Signature	Date
Prepared by:	R. Samadi		29.09.2015
Verified by:			
Approved by:			
Approved by:			

Document Change Record

Issue	Rev.	Date	Pages affected	Modification	DCR	Initials
1.0	0.0	15.06.2015		Initial version		
1.0	1.0	29.09.2015		Eq. 13 corrected		

DCR=Document Change Request

Contents

1 Introduction 3
2 General principle 3
3 White noise 3
4 Stellar granulation 4
5 Solar-like oscillations 4

5.1 Universal pattern 5
5.2 Theoretical set of mode frequencies 7

6 Illustration **8**
6.1 Universal pattern 8
6.2 A theoretical set of mode frequencies 8

1 Introduction

The Stellar Light-curve Simulator (SLS) aims at simulating stochastically-excited oscillations together with stellar granulation background and white noise. It allows the simulation of two different types of oscillation spectra: i) oscillation spectra computed on the basis of the so-called Universal Pattern by Mosser et al. [16]) including in option mixed-modes following the asymptotic gravity mode spacing [19]. ii) oscillation spectra computed using a given set of theoretical frequencies pre-computed with the ADIPLS code [9].

2 General principle

The stochastic nature of the different simulated phenomenon (i.e. white noise, stellar granulation and stochastically-excited oscillations) are simulated following Anderson et al. [1, see also Baudin et al. [4]]. As detailed below, the properties of the simulated stellar signal are first modelled in the Fourier domain, we next add a random noise to simulate the stochastic nature of the signal, and finally we perform an inverse Fourier transform to come back in the time domain and derive the corresponding time-series (light-curve).

Let $\mathcal{F}(\nu)$ be the Fourier Transform of the simulated light-curve $\mathcal{S}(t)$, and $\overline{\mathcal{P}}(\nu)$ the expectation of the Power Spectral Density (PSD) associated with the stellar signal (i.e. the PSD one would have in average over an infinite number of realisations). If the frequency bins of the PSD are un-correlated, we can show then that

$$\mathcal{F}(\nu) = \sqrt{\overline{\mathcal{P}}}\ (u + \mathcal{I}\, v)\ , \tag{1}$$

where u, and v are two un-correlated Normal distributions of mean zero and variance unit, and $\mathcal{I}$ is the imaginary unit ($\mathcal{I}^2 = -1$). We finally compute the inverse Fourier Transform of $\hat{F}(\nu)$ to derive the the simulated light-curve $\mathcal{S}(t)$ for a given realisation. Note that the PSD $\mathcal{P}(\nu)$ associated with a given realisation verifies

$$\mathcal{P}(\nu) = |\mathcal{F}(\nu)|^2 = \overline{\mathcal{P}}\ \left(u^2 + v^2\right)\ . \tag{2}$$

Our PSD is "single-sided", which means that the integral of the PSD from $\nu = 0$ (excluded) to the Nyquist frequency is equal to the variance of the time-series.

The expectation $\overline{\mathcal{P}}(\nu)$ is here the sum of a white noise component W, granulation background $G(\nu)$, and the oscillations spectrum $O(\nu)$, that is

$$\overline{\mathcal{P}}(\nu) = W + G(\nu) + O(\nu)\,. \tag{3}$$

Consistently with our initial hypothesis, all these components are by construction un-correlated. We describe in the following the way each component is modelled.

3 White noise

The white noise is supposed to be composed by the contribution of the shot-noise (photon noise) and a non-photonic contribution (instrumental component). If P is the level of the shot noise and N that of the non-photonic noise in the PSD, the total level of the white noise in the PSD is then

$$W = P + N\,. \tag{4}$$

The variance of the shot noise varies as the photon counts, and hence proportionally to the star flux. Let P_0 be the reference level of the shot noise in the PSD (in ppm^2/Hz). The stellar flux being related to the stellar magnitude V by

$$F = F_0\, 10^{0.4\ (V_0 - V)}\,, \tag{5}$$

Instrument	Reference magnitude (V_0)	P_0 ppm$^2/\mu$Hz	$\sigma_{P,0}$ ppm per hour
CoRoT - seismology channel	6	0.42	7.7
PLATO - 2 F-cameras	8	26.3	60.5
PLATO - 32 N-cameras	11	5.25	27
Kepler	12	8.3	34

Table 1: Reference photon noise levels of different instruments in terms of white noise in the power spectrum (P_0) and standard deviation at a sampling time of 1 hour ($\sigma_{P,0}$).

the level of shot noise is related to the star magnitude according to

$$P = P_0\, 10^{0.4\,(V-V_0)}\,. \tag{6}$$

For CoRoT the reference photon noise level is $P_0 = 0.42$ ppm$^2/\mu$Hz at the reference magnitude $V_0 = 6$. Note that for a single sided spectrum, a reference white noise level of P_0 in the power spectrum corresponds to a standard deviation of $\sigma_{P,0} = \sqrt{(W/2)\,10^6/3600}$ at a sampling time of one hour. For CoRoT, this correspond to $\sigma_{P,0} = 7.7$ ppm per hour. Table 1 reports the reference photon noise levels of different instruments. Concerning the non-photonic noise, the latter is supposed to scale as the star flux, and accordingly its level in the PSD scales as

$$N = N_0\; 10^{0.8\,(V-V_0)}\,, \tag{7}$$

where N_0 is the reference level of the non-photonic noise (i.e. specified at the reference magnitude V_0).

4 Stellar granulation

The granulation background is simulated by assuming two pseudo-Lorenztian functions

$$G(\nu) = \sum_{i=1,2} \frac{h_i}{1 + (2\pi\tau_i\nu)^{\alpha_i}}\,, \tag{8}$$

where h_i is the height, τ_i the characteristic time-scale, and α_i the slope of the Lorenztian function. The values of h_i and τ_i are determined from the scaling relations established by Kallinger et al. [14] with Kepler observations of red giants, sub-giants and main-sequence stars. These scaling relations are function of peak frequency $\nu_{\rm max}$ of the oscillations and the stellar mass M. Following Kallinger et al. [14], the values of the two slopes (α_1 and α_2) are both fixed to four.

5 Solar-like oscillations

Each individual resolved mode of frequency ν_i is described by Lorentzian profile

$$\mathcal{L}_i(\nu) = \frac{H_i}{1 + \left(2\,(\nu-\nu_i)\,/\Gamma_i\right)^2}\,, \tag{9}$$

where H_i is the mode height, and Γ_i its linewidth. Unresolved modes are modelled using the following profile [see, e.g. 8]

$$\mathcal{L}_i(\nu) = \frac{\pi\,\Gamma_i\,H_i}{2\delta\nu}\,\mathrm{sinc}^2\left[\pi\,(\nu-\nu_i)\right] \tag{10}$$

where $\delta\nu$ is the resolution of the spectrum. Finally, the oscillation spectrum is the sum over the different modes included

$$\mathcal{O}(\nu) = \sum_i \mathcal{L}_i(\nu)\,. \tag{11}$$

Depending of the choice of the user, the mode heights, linewidths and frequencies can be determined by two different methods. One of this method relies on the so-called Universal Pattern [16] while the second relies on a set of theoretical mode frequencies computed with the ADIPLS adiabatic pulsation code. We describe below these two methods.

5.1 Universal pattern

Each mode frequency $\nu_{n,\ell}$ is computed according to the Universal Pattern proposed by Mosser et al. [16]

$$\nu_{n,\ell} = n + \frac{\ell}{2} + \varepsilon(\Delta\nu) - d_{0\ell}(\Delta\nu) + \frac{\alpha_\ell}{2}\left(n - \frac{\nu_{\max}}{\Delta\nu}\right)^2 \Delta\nu + \delta_{n,\ell}\,, \tag{12}$$

where n and ℓ are respectively the radial order and the degree of a given mode, ε is an offset, $d_{0\ell}$, the small separation, α_ℓ the curvature, $\Delta\nu$ is the large separation, and finally the term $\delta_{n,\ell}$ accounts for a possible coupling with the gravity modes, which results in the deviation of the mode frequency from its uncoupled solution ("pure" acoustic mode) and gives the mode its mixed-mode nature. For a dipole mode, $\delta_{n,\ell}$ is computed according to the asymptotic gravity-mode spacing [19]

$$\delta_{n,\ell} = \frac{\Delta\nu}{\pi}\arctan\left[q\tan\pi\left(\frac{1}{\Delta\Pi_1\nu_{n,\ell}} - \epsilon_g\right)\right]\,, \tag{13}$$

where q is the coupling coefficient, $\Delta\Pi_1$ the asymptotic period spacing of the (pure) dipole g modes, and ϵ_g is an offset fixed here to zero. For a radial modes obviously $\delta_{n,0} = 0$, while for all modes with angular degree $\ell \geq 2$ we neglect the deviation and assume $\delta_{n,\ell} = 0$.

The variation of the mode heights with frequency are modelled with a Gaussian envelope $G(\nu)$, centered at $\nu_{\max}$

$$G(\nu) = \exp\left[\frac{-(\nu - \nu_{\max})^2}{\delta\nu_{\rm env}^2/4\ln 2}\right]\,, \tag{14}$$

where $\delta\nu_{\rm env}$ is the full width at half maximum, which is supposed to scale as [18]:

$$\delta\nu_{\rm env} = 0.66\,\nu_{\max}^{0.88}\,. \tag{15}$$

Accordingly, the mode height of each given mode (n,ℓ,m) is given by

$$H_{n,\ell} = G(\nu_{n,\ell})\,V_l^2\,H_{\max}\,, \tag{16}$$

where V_l, is mode visibility determined from Mosser et al. [18] and $H_{\max}$ is the maximum of the mode heights derived from the scaling relation established by Mosser et al. [20], that is

$$H_{\max} = \alpha\,\nu_{\max}^{-2.38} \tag{17}$$

where $\alpha = 2.03\ 10^8$ is an had-doc scaling parameter tuned such as to have mode height compatible with CoRoT observations.

Concerning the mode linewidths $\Gamma_{n,\ell}$, they are supposed to be constant with frequency. This constant value is determined from the theoretical scaling relations of Belkacem [6], which is only function of the effective temperature, $T_{\rm eff}$ as follows

$$\Gamma_{\max} = \Gamma_{\max,0}\left(\frac{T_{\rm eff}}{4800\ {\rm K}}\right)^{10.8}\,, \tag{18}$$

where $\Gamma_{\max,0} = 0.19$ μHz. The dipolar mixed modes have, however, a much smaller linewidths than their associated "pure" acoustic modes. This is mainly because their inertia is much larger as a consequence of the fact they behave as gravity in the inner layers. Indeed, the mode linewidth scales as the inverse of the mode inertia [see, e.g., 7]. Let $I^m_{n,\ell}$ (resp. $\Gamma^{(m)}_{n,\ell}$) be the mode inertia (resp. mode linewidth) of a dipolar mixed-modes and $I^0_{n,\ell}$ (resp. $\Gamma^{(0)}_{n,\ell}$) this of the "pure" acoustic mode of same radial order, we have then

$$\Gamma^{(m)}_{n,\ell} = \Gamma^{(0)}_{n,\ell} \left(\frac{I^0_{n,\ell}}{I^m_{n,\ell}} \right) , \tag{19}$$

where according to our previous assumption $\Gamma^{(0)}_{n,\ell} = \Gamma_{\max}$ for all couple (n,ℓ). Now, according to Goupil et al. [13],

$$\frac{I^0_{n,\ell}}{I^m_{n,\ell}} \simeq 1 - \frac{I_{\rm core}}{I} = 1 - \zeta \tag{20}$$

where $I_{\rm core}$ is the contribution of the core to the mode inertia, and ζ is defined as

$$\zeta = \frac{1}{1 + \alpha_0 \, \chi^2} \tag{21}$$

$$\chi = 2 \left(\frac{\nu_{n,\ell}}{\Delta\nu} \right) \cos \left(\frac{\pi}{\Delta\Pi_1 \, \nu_{n,\ell}} \right) \tag{22}$$

$$\alpha_0 = \Delta\nu \, \Delta\Pi_1 \tag{23}$$

The oscillation spectrum is then constructed by summing the Lorentzian profile of each modes. We include modes from the radial order $n = 1$ up to the radial order $n = \text{integer } (\nu_c/\Delta\nu)$ where ν_c is the cuttoff-frequency (see Eq. 28) and from the angular degree $\ell = 0$ to $\ell = 3$.

The simulator requires three main input parameters, $\nu_{\max}$, $T_{\rm eff}$ and $\Delta\nu$, from which all the other parameters are established using scaling relations, except $\Delta\Pi_1$ and q which can be provided as optional inputs (otherwise no mixed modes are included). In case $\Delta\nu$ is not provided, it is computed according to the scaling relation [20]

$$\Delta\nu = 0.274 \, \nu^{0.757}_{\max} \tag{24}$$

The stellar mass used for the granulation scaling relations is determined by combining the scaling relation for $\nu_{\max}$ [see 6, and reference therein]

$$\nu_{\max} = \nu_{\max,\odot} \, \frac{g}{g_\odot} \sqrt{\frac{T_{\rm eff,\odot}}{T_{\rm eff}}} , \tag{25}$$

with the scaling relation for $\Delta\nu$

$$\Delta\nu = \Delta\nu_\odot \sqrt{\frac{M}{R^3}} \tag{26}$$

where g is surface gravity, $\log g_\odot = 4.438$, $T_{\rm eff,\odot} = 5777$ K, $\nu_{\max,\odot} = 3100$ μHz, and $\Delta\nu_\odot = 135$ μHz. Indeed, combining the two scaling relations yields [see, e.g., 17]

$$m = M_\odot \left(\frac{\nu_{\max}}{\nu_{\max,\odot}} \right)^3 \left(\frac{\Delta\nu}{\Delta\nu_\odot} \right)^{-4} \left(\frac{T_{\rm eff}}{T_{\rm eff,\odot}} \right)^{3/2} . \tag{27}$$

Finally, the cutoff frequency ν_c is derived from the following scaling relation

$$\nu_c = \nu_{c,\odot} \, \frac{g}{g_\odot} \sqrt{\frac{T_{\rm eff,\odot}}{T_{\rm eff}}} , \tag{28}$$

where $\nu_{c,\odot} = 5300$ μHz.

5.2 Theoretical set of mode frequencies

The oscillation spectrum is directly constructed using a set of theoretical eigenfrequencies computed with the ADIPLS code [9]. The program allows one to including constant mode spilling given as input the surface rotation period $T_{rot} = 2\pi/\Omega_{\rm surf}$ where $\Omega_{\rm surf}$ is the surface rotation rate. The set of frequencies including in the model are

$$\nu^{(0)}_{n,\ell,m} = \nu_{n,\ell} + \frac{m}{T_{rot}} \, (1 - c_{n,\ell}) \tag{29}$$

where m is the azimuthal order, and $c_{n,\ell}$ is the Ledoux's constant [21, see, e.g.] provided by ADIPLS. We considered all the modes of radial order $n \geq 1$ up to the cutoff frequency and consider modes with angular degrees ranging from $\ell = 0$ to $\ell = 3$ (included). Near-surface effects are eventually added as follows

$$\nu_{n,\ell,m} = \nu^{(0)}_{n,\ell,m} + a\,\nu_{\rm max} \left(1 - \frac{1}{1 + \left(\nu^{(0)}_{n,\ell,m} / \nu_{\rm max} \right)^b} \right) , \tag{30}$$

where a and b are two free parameters, which are given as inputs to the program.

The mode height of each given mode is computed according to

$$H_{n,\ell,m} = G(\nu_{n,\ell}, m)\, V_l^2\, r^2_{n,\ell,m}(i)\, H_{\rm max} \tag{31}$$

where G is the Gaussian envelope defined in Eq. (14), V_l the mode visibility (same values than those used with the universal pattern), $H_{\rm max}$ the mode height a the peak frequency, and $r_{n,\ell,m}$ is the (relative) visibility of a multiplet of azimuthal order m for a given inclination angle i. The ratio $r_{n,\ell,m}$ is computed according to Dziembowski [11, see also Gizon & Solanki [12]] and represents – at fixed value of n and ℓ – the ratio of the mode height for a given inclination angle i to the mode height at the angle i=0 degree.

Since the mode linewidth is inversely proportional to the mode inertia, we model it as

$$\Gamma_{n,\ell,m} = \Gamma_{\rm max} \left(\frac{I_{\rm max}}{I_{n,\ell}} \right) \gamma(\nu_{n,\ell,m}) \, , \tag{32}$$

where $I_{n,\ell}$ is the mode inertia, $I_{\rm max}$ is the mode inertia of the radial modes interpolated at $\nu = \nu_{\rm max}$, $\Gamma_{\rm max}$ is the mode linewidth at $\nu = \nu_{\rm max}$ derived from tow different scaling relations (see below), and the function $\gamma(\nu)$ models in an empirical way the existence of a plateau. The latter is defined as follows

$$\gamma(\nu) = 1 + A \, (1 - G'(\nu)) \tag{33}$$

where $G'(\nu)$ is a Gaussian function defined as in Eq. (14) but with a width two times larger, that is $\delta\nu'_{\rm env} = 2\delta\nu_{\rm env}$, where $\delta\nu_{\rm env}$ is given by the scaling relation of Eq. (15).

The mode linewidth a the peak frequency, $\Gamma_{\rm max}$, is determined on the basis of the scaling relation derived by Appourchaux et al. [2] from main-sequence Kepler targets, i.e.

$$\Gamma_{\rm max} = \Gamma_{\rm max,0} + \beta \left(\frac{T_{\rm eff}}{T_{\rm eff,\odot}} \right)^s , \tag{34}$$

where $\Gamma_{\rm max,0} = 0.20\,\mu$Hz, $\beta = 0.97$, and $s = 13.0$.

For a single-side PSD, the mode height is related to the mode linewidth as [see, e.g. 5][1]

$$H_{\rm max} = \frac{2\,A^2_{\rm max}}{\pi\,\Gamma_{\rm max}} \tag{35}$$

[1] The additional factor two comes from the fact we assume here as single-side PSD while Baudin et al. [5] assumed a double-sided PSD.

$T_{\rm eff}$	$\nu_{\rm max}$	$\Delta\nu$	$\Delta\Pi$	q
K	μHz	μHz	s	
4800	61.2	5.72	232.2	0.27

Duration	Sampling	Magnitude	Noise level	Reference magnitude
days	s		ppm per hour	
150	512	12	7.7	6

Table 2: Parameters of the simulation displayed in Fig. 2.

where $A_{\rm max}$ is the *rms* of the mode amplitude at the peak frequency. The latter is related to the bolometric amplitude $A_{\rm max,bol}$ using the correction proposed for Kepler spectral band by Ballot et al. [3]

$$A_{\rm max} = A_{\rm max,bol} \left(\frac{T_{\rm eff}}{5934 \text{ K}} \right)^{-0.8} . \quad (36)$$

Note that the CoRoT spectral band results in very similar corrections [see 15]. Finally, $A_{\rm max,bol}$ is derived from the scaling relations derived by Corsaro et al. [10] and defined as

$$\begin{aligned} \ln(A_{\rm max,bol}) \quad = \quad & \ln(A_{\rm max,bol,\odot}) + (2s - 3t) \ln(\nu_{\rm max}/\nu_{\rm max,\odot}) + \\ & (4t - 4s) \ln(\Delta\nu/\Delta\nu_{\odot}) + (5s - 1.5t - r + 0.2) \ln(T_{\rm eff}/T_{\rm eff,\odot}) + \ln(\beta) \end{aligned} \quad (37)$$

where $A_{\rm max,bol,\odot} = 2.53$ ppm (rms) is the maximum of the bolometric solar mode amplitude [15], and s, t, r and β are coefficients that depends on the star evolutionary status (see Table 3 & 4 in Corsaro et al. [10]).

6 Illustration

6.1 Universal pattern

The Fig. 1 show the theoretical spectrum obtained with the method based on the Universal Pattern. Figure 2 presents the power spectrum generated from the theoretical spectrum shown. The parameters of this simulations are given in Table 2.

6.2 A theoretical set of mode frequencies

The Fig. 3 presents the theoretical spectrum derived from a theoretical set of eigenfrequencie. Figure 4 shows the power spectrum generated from the theoretical spectrum. The parameters of this simulations are given in Table 3.

References

[1] Anderson, E. R., Duvall, T. L., & Jefferies, S. M. 1990, ApJ, 364, 699

[2] Appourchaux, T., Benomar, O., Gruberbauer, M., et al. 2012, A&A, 537, A134

[3] Ballot, J., Gizon, L., Samadi, R., et al. 2011, A&A, 530, A97

[4] Baudin, F., Samadi, R., Appourchaux, T., & Michel, E. 2007, ArXiv e-prints

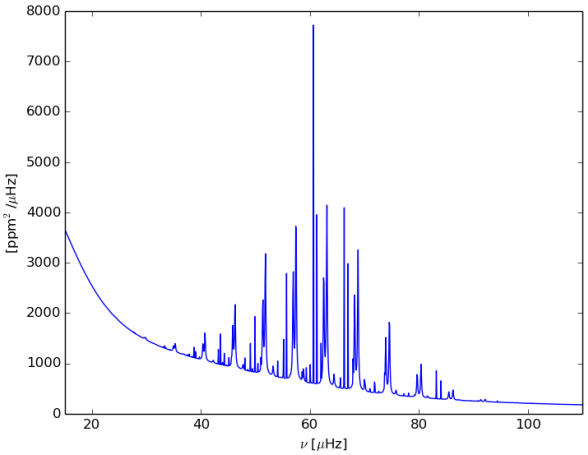

Figure 1: Theoretical spectrum (expectation) derived with the method based on the Universal Pattern.

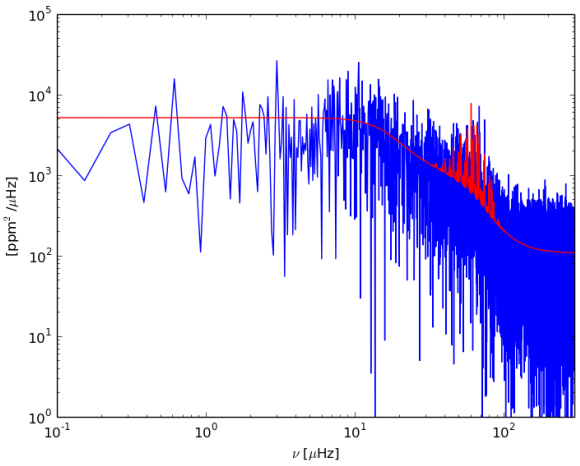

Figure 2: The blue curve correspond to the simulated power spectrum (i.e. a given realisation) generated with the method based the Universal Pattern and the red curve corresponds to the associated theoretical spectrum (expectation).

$T_{\rm eff}$ K	$\nu_{\rm max}$ μHz	$\Delta\nu$ μHz	Mass	radius
5954	2027	95.1	1.182	1.335

Duration days	Sampling s	Magnitude	Noise level ppm per hour	Reference magnitude
150	512	6	7.7	6

Table 3: Parameters of the simulation displayed in Fig. 4.

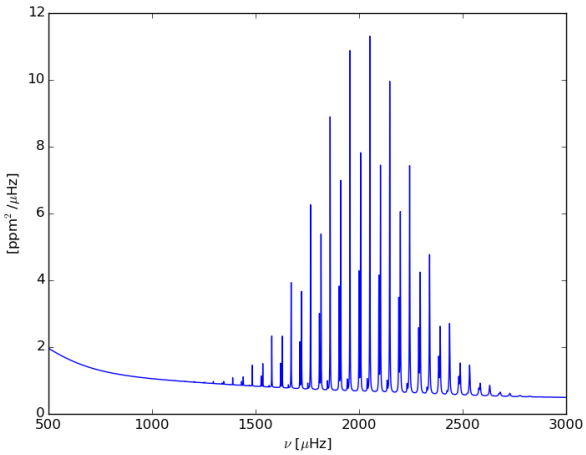

Figure 3: Theoretical spectrum (expectation) derived with the method relying on a input set of theoretical frequencies computed with ADIPLS.

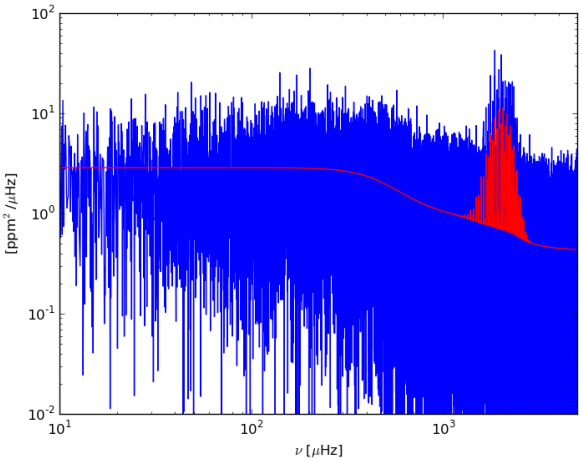

Figure 4: The blue curve correspond to the simulated power spectrum (i.e. a given realisation) generated the method relying on a input set of theoretical frequencies computed with ADIPLS and the red curve corresponds to the associated theoretical spectrum (expectation).

[5] Baudin, F., Samadi, R., Goupil, M.-J., et al. 2005, A&A, 433, 349

[6] Belkacem, K. 2012, in SF2A-2012: Proceedings of the Annual meeting of the French Society of Astronomy and Astrophysics, ed. S. Boissier, P. de Laverny, N. Nardetto, R. Samadi, D. Valls-Gabaud, & H. Wozniak, 173–188, arXiv:1210.3505

[7] Belkacem, K. & Samadi, R. 2013, in Lecture Notes in Physics, Berlin Springer Verlag, Vol. 865, Lecture Notes in Physics, Berlin Springer Verlag, ed. M. Goupil, K. Belkacem, C. Neiner, F. Lignières, & J. J. Green, 179

[8] Berthomieu, G., Toutain, T., Gonczi, G., et al. 2001, in ESA SP-464: SOHO 10/GONG 2000 Workshop: Helio- and Asteroseismology at the Dawn of the Millennium, 411–414

[9] Christensen-Dalsgaard, J. 2008, Ap&SS, 316, 113

[10] Corsaro, E., Fröhlich, H.-E., Bonanno, A., et al. 2013, MNRAS, 430, 2313

[11] Dziembowski, W. A. 1971, Acta Astron., 21, 289

[12] Gizon, L. & Solanki, S. K. 2003, ApJ, 589, 1009

[13] Goupil, M. J., Mosser, B., Marques, J. P., et al. 2013, A&A, 549, A75

[14] Kallinger, T., De Ridder, J., Hekker, S., et al. 2014, A&A, 570, A41

[15] Michel, E., Samadi, R., Baudin, F., et al. 2009, A&A, 495, 979

[16] Mosser, B., Belkacem, K., Goupil, M. J., et al. 2011, A&A, 525, L9

[17] Mosser, B., Belkacem, K., Goupil, M.-J., et al. 2010, A&A, 517, A22

[18] Mosser, B., Elsworth, Y., Hekker, S., et al. 2012, A&A, 537, A30

[19] Mosser, B., Goupil, M. J., Belkacem, K., et al. 2012, A&A, 540, A143

[20] Mosser, B., Samadi, R., & Belkacem, K. 2013, ArXiv e-prints

[21] Unno, W., Osaki, Y., Ando, H., Saio, H., & Shibahashi, H. 1989, Nonradial oscillations of stars (Tokyo: University of Tokyo Press, 1989, 2nd ed.)